Original Research Article

Influence of 3D Printing Filament Properties on Rebound Performance of Airless Tennis Balls

Ian Seungbin Shin

University High School, 601 Gregory St, Normal, IL 61790, United States

ABSTRACT

Traditional sports balls use an internal pressurized rubber core for bounce but suffer from pressure loss and limited lifespan. Airless sports balls replace this core with a rubber or plastic lattice structure, mitigating these issues. This study examines material properties influencing the rebound performance of airless tennis balls, using seventeen 3D printing filaments in a standardized design compared against a regulation pressurized ball. Mechanical properties (Young's modulus, tensile strength, elongation at break, and impact strength) were sourced from manufacturer datasheets, while damping behavior was measured via free-vibration decay of printed cantilever beams. Each filament had one cantilever beam with three filmed trials, averaged for analysis. Rebound performance was evaluated through coefficient of restitution (COR) and rebound reliability (success rate) across repeated drop tests, which were continued until three vertical rebounds were achieved. Results show damping time as the strongest predictor of COR, with longer damping times yielding higher values. Rebound reliability correlated negatively with Young's modulus and tensile strength, suggesting that moderate stiffness and strength favor consistent vertical rebounds. Impact strength was linked to durability, with low values correlating with fracture under repeated impact. A performance map plotting COR against rebound reliability identified optimal filament candidates for replicating pressurized ball performance, excluding fragile filaments. Materials with moderate stiffness, low damping, and high impact strength demonstrated the best balance of rebound magnitude, consistency, and durability. Future work should investigate filament blending to optimize stiffness and damping, lattice geometry effects, and long-term durability.

Keywords: Coefficient of Restitution (COR); 3D printing filaments; Rebound Performance; Impact Strength; Damping Properties; Young's Modulus

INTRODUCTION

Traditional sports balls utilize internal air pressure to achieve their desired rebound characteristics (1, 2). There are several issues that arise from this dependence– loss of pressure over time, the need for airtight enclosure, and environmental waste from discarded balls. Recently, alternatives have begun to emerge that replace the internal pressurized core with engineered lattice structures. The most prevalent recent example is Wilson's Airless Gen1 Basketball, released in 2023 (3), which replicates the bounce of a traditional pressurized basketball without the use of internal air pressure. Although the structural design is public, the specific material and mechanical properties are still undisclosed.

Corresponding author: Ian Seungbin Shin, E-mail: iansshin7@gmail.com.

Accepted October 8, 2025
https://doi.org/10.70251/HYJR2348.35738746

The concept of an airless ball has attracted interest among engineers and sports enthusiasts, particularly with balls where consistent rebound is critical, such as tennis balls or basketballs. Various online forums have conducted informal experiments, which explore 3D printing with filaments such as PLA, PETG, and TPU to replicate pressurized-ball performance (4, 5). However, most of these efforts are qualitative, and there's still limited understanding as to how specific mechanical properties influence rebound performance.

This study addresses that gap by investigating the effect of 3D printing filament properties on the performance of airless tennis balls. A standardized lattice geometry was created among 17 different commercially available 3D printing filaments, and bounce performance was measured and compared with that of a regulation pressurized tennis ball. Performance evaluation was based on the coefficient of restitution (COR), which measures the ratio of rebound velocity to initial velocity and essentially measures the energy retained in a material after impact (6). While COR is already known to depend on multiple factors (7, 8)—including material stiffness, damping, and density, previous studies have not isolated material effects under controlled conditions. In this work, geometry, impact speed, and ambient temperature were held constant to identify correlations between filament properties and rebound performance. The results of this investigation provide a quantitative basis for material selection in the design of airless sports balls in the future and can help inform future development of advanced sports technology.

METHODS AND MATERIALS

Filaments and Mechanical properties

The airless tennis ball design used in this investigation was the Airless Tennis Ball 2.0 Pickleball Wiffle model, designed by filete3d and publicly available on MakerWorld (9). All samples were printed using a Bambu Lab P1S 3D printer, following the manufacturer's recommended nozzle temperature, bed temperature, and print speed for each filament to ensure consistency.

Seventeen commercially available 3D printing filaments were utilized in this study, fifteen of which were purchased from Bambu Lab. From Bambu Lab, the following were obtained: PLA category (PLA Basic, PLA CF; general-purpose, easy-printing materials with moderate strength), PETG category (PETG HF, PETG CF; good toughness, chemical resistance, and dimensional stability), ABS/ASA category (ABS, ABS GF, ASA, ASA CF; engineering thermoplastics with higher heat resistance and weatherability), PC/TPU category (PC, TPU 95A, TPU AMS; PC offers high strength and heat resistance, TPU is flexible with high impact absorption), and PA/PET category (PA6 CF, PA6 GF, PAHT CF, PET CF; high-strength, wear-resistant materials with good thermal performance). GF indicates a glass fiber filament, while CF indicates a carbon fiber filament. BIQU PLA-HR flexible filament– marketed directly as a filament for airless sports ball production– was purchased from BIQU. Finally, PEBA-S filament, a thermoplastic high-performance elastomer, was purchased from Kimya. The filaments' mechanical properties—Young's modulus, tensile strength, breaking elongation rate, and impact strength—were obtained from the manufacturers' datasheets.

Figure 1a presents an Ashby-style plot (10) of tensile strength versus Young's modulus. In general, a higher Young's modulus correlated with a higher tensile strength, indicating that high material stiffness correlates with an increased resistance to stretching forces. CF or GF filaments appear to trend towards higher stiffness and tensile strength. CF filaments appear to cluster in the upper-right region of the plot, reflecting both the high rigidity and tensile strength provided by the stiff carbon fibers (11). GF filaments appear to trend in the same way, but generally have a lower increase in tensile strength, which is consistent with the lower intrinsic strength of glass fibers compared to carbon fibers (12).

Figure 1b shows tensile strength versus breaking elongation rate, displaying an expected trade-off between stiffness and ductility (13). The addition of CF or GF reduces ductility substantially, as the rigid fibers limit deformation and promote earlier fracture initiation.

The damping, or energy dissipation of each filament was not provided by manufacturers. To measure damping behavior, thin beams (10 mm × 100 mm × 3 mm) were printed from each filament and clamped at one end. The free end was displaced by a fixed amount, before being released (14). Only one beam was used for each of the three trials. The oscillation period—from release to the absence of visible motion—was measured from high-frame-rate video (240 frames / sec) recorded using a smartphone (Figure 2). The measured duration, referred to here as damping time, provides a qualitative measure of the relative damping capability of each

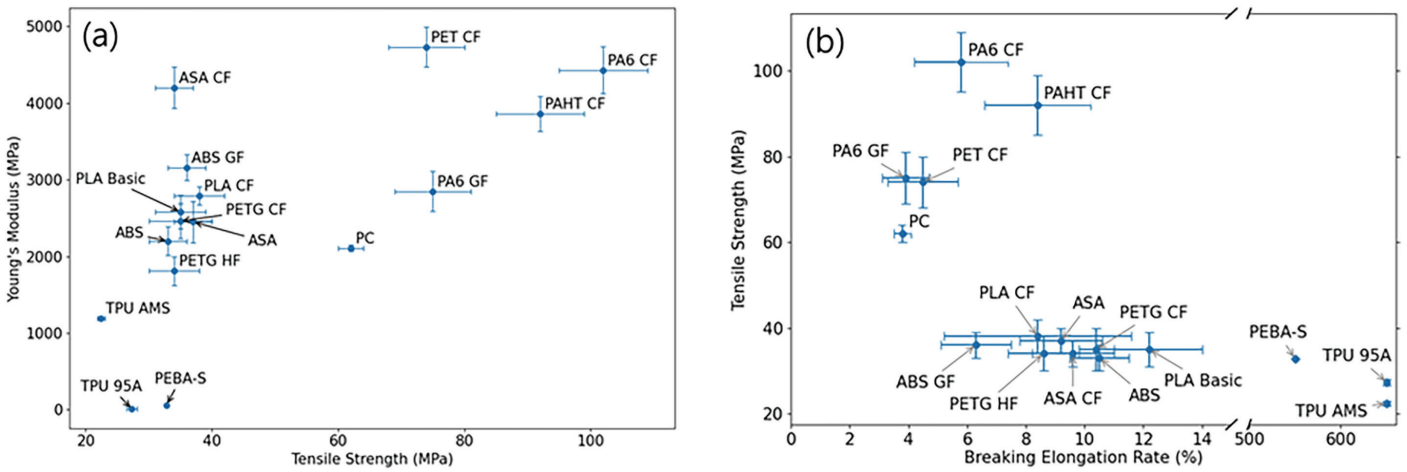

Figure 1. Comparisons between mechanical properties of 3D printing filaments: (a) Young's modulus vs. tensile strength; (b) tensile strength vs. breaking elongation rate. Young's modulus is used as a measure of a material's stiffness— the amount of tension they can undergo in a certain direction before deformation. Tensile strength measures the amount of tension a material can undergo in a certain direction before complete fracture. Breaking elongation rate is used as a measure of a material's flexibility— the percentage of stretch a material can achieve in a tensile before fracturing.

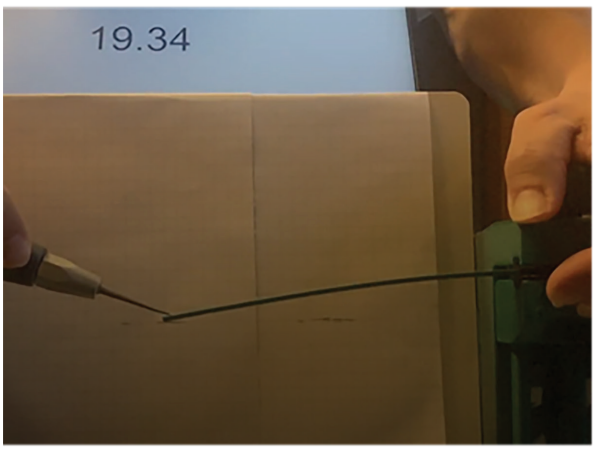

Filaments	Avg. damping time (sec)	Filaments	Avg. damping time (sec)
ABS	2.98 ± 0.08	PEBA-S	11.99 ± 0.06
ABS GF	2.29 ± 0.09	PET CF	2.21 ± 0.09
ASA	2.60 ± 0.03	PETG HF	3.47 ± 0.06
ASA CF	2.08 ± 0.07	PETG CF	2.35 ± 0.08
BIQU	4.43 ± 0.33	PLA Basic	2.92 ± 0.16
PA6 CF	1.63 ± 0.02	PLA CF	1.99 ± 0.02
PA6 GF	1.52 ± 0.02	TPU 95A	1.17 ± 0.02
PAHT CF	1.68 ± 0.02	TPU AMS	1.35 ± 0.04
PC	2.96 ± 0.16		

Figure 2. Example of damping test setup and average damping times for each 3D printing filament. Thin beams (10 mm × 100 mm × 3 mm) of each filament are clamped at one end. The free end was displaced by a fixed amount, before being released. The damping times were evaluated by oscillation period—from release to the absence of visible motion—and were measured from high-frame-rate video (240 frames / sec) recorded using a smartphone.

filament. Overall, the addition of CF or GF tended to reduce damping time, indicating lower inherent energy dissipation. This trend is consistent with the role of short fiber reinforcement in constraining polymer chain mobility and increasing stiffness. In contrast, BIQU and PEBA-S exhibited notably longer damping times, reflecting their more flexible, energy-absorbing characteristics.

Rebound Testing

Rebound performance was evaluated by measuring the COR of each ball. Balls were released from three different heights—3 ft (0.91 m), 5 ft (1.52 m), and 7 ft (2.13 m)—onto a concrete pad (Figure 3a). Balls were released without any spin or additional forces applied. While four balls were printed for each filament, the same ball was used for each of the trials, until a

ball experienced a fracture. A trial was considered a successful rebound if the rebound was nearly completely vertical, to ensure accurate height measurements.

COR was calculated as:

$$COR = \sqrt{\frac{h_r}{h_0}}$$

where h_r is rebound height and h_0 is initial drop height (15). For each ball type, trials were repeated until three successful rebounds at each height were obtained. Rebound reliability was measured by success rate, which was calculated as:

$$Success\ rate = \frac{Number\ of\ successful\ trials}{Total\ trials} \times 100\%$$

Deviation from official tennis ball COR ranges was assessed by calculating the root-mean-square deviation (RMSD) of each ball. RMSD was calculated as:

$$RMSD(|COR - C|) = \sqrt{\frac{1}{n}\sum_{i=1}^{n}(COR_i - C)^2}$$

where C is the central value of the official International Tennis Federation (ITF) COR range, and n is the number of trials. The RMSD in this case represents the average deviation of each trial from the official ITF COR value.

RESULTS

Figure 3b displays the COR results for a regulation pressurized tennis ball, taken directly from a sealed can before testing. The dashed red lines denote the official ITF (International Tennis Federation) acceptable COR range for tennis balls. The three measured COR values from each height all fell into this official range, confirming the validity of the measurement methodology. The percentage value beneath each set of drop height trials represents the success rate for each drop height. The tennis ball consistently rebounded vertically, achieving success rates of 100% for 3 ft and 5 ft drops, and 75% for the 7 ft drop.

Figures 4a and 4b display COR values for airless tennis balls made from non-reinforced and fiber-reinforced filaments, respectively. For non-reinforced filaments (Figure 4a), PLA Basic and ABS achieved the closest COR values to the reference, with relatively high success rates. TPU 95A and TPU AMS had high success rates across all heights, but substantially lower COR, suggesting excellent rebound reliability but low energy restitution. PETG HF and PC exhibited variable COR and lower success rates, especially at intermediate heights. For fiber-reinforced filaments (Figure 4b), most had reduced success rates compared to non-reinforced

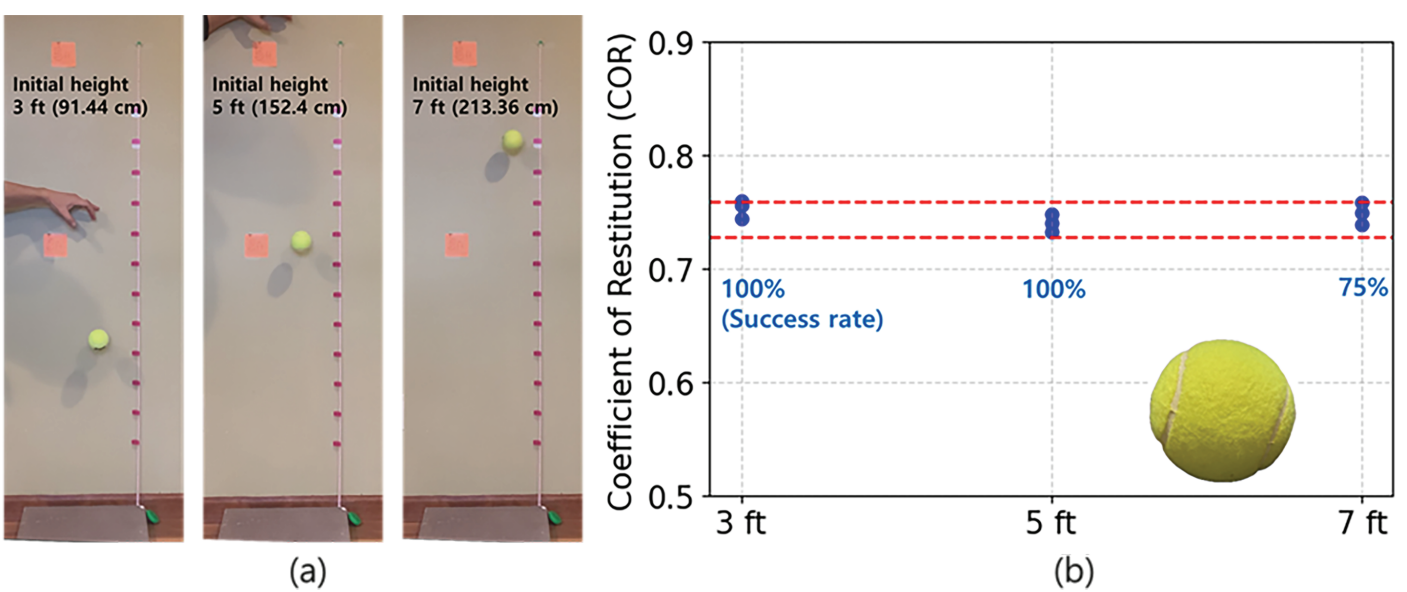

Figure 3. (a) Rebound test configuration for COR measurement across drop heights of 3ft, 5f, and 7ft; (b) COR and success rate of a regulation pressurized tennis ball across drop heights of 3ft, 5ft, and 7ft.

versions. PA6 CF, PETG CF, and ASA CF showed both lower COR and reduced success rates at higher drop heights compared to their non-reinforced counterparts.

To quantitatively assess deviation from the official reference COR range for each ball, the RMSD was calculated for each ball. Smaller RMSD values indicate results more precisely clustered around the central ITF COR value. For the tennis ball, the calculated RMSD(|COR−C|) was 0.0047, showing the measured COR values were tightly clustered around the ITF reference center value.

Figure 5a ranks the materials by RMSD(|COR−C|) from lowest to highest, or most accurate to least accurate. PAHT CF, PA6 GF/CF, and PLA Basic have the smallest deviations from the tennis ball, while TPU 95A and TPU AMS have the largest. Figure 5b ranks the same materials by their average success rate across drop heights, from highest to lowest. TPU 95A, PLA Basic, and PET CF achieved the highest success rates, and PA6 CF and PETG CF the lowest. Figure 5c plots each ball's average success rate against their RMSD(|COR−C|). The most successful balls are thus represented by the balls which have the lowest RMSD(|COR−C|) and the highest average success rate. These balls are clustered in the top left corner of the plot, with the tennis ball being the one closest to the top left corner.

DISCUSSION

Study Limitations

This study has several key limitations. First, all data was derived from short-term testing conducted within a few hours, which limits the ability to assess longer-term performance or durability. Second, potential confounding variables were not fully controlled. For example, the progressive wear of filament balls during rebound testing was not accounted for, and other uncontrolled factors may have influenced results. Finally, the relatively small scale of the experiment may have introduced variability in the data. Despite these limitations, the results provide meaningful insights and the conclusions drawn are significant.

Correlations between Mechanical Properties and Performance

Figure 6a shows the correlation between a filament's average damping time and its average COR. A weak but generally positive trend was observed. Filaments with longer damping times, indicating lower energy loss per

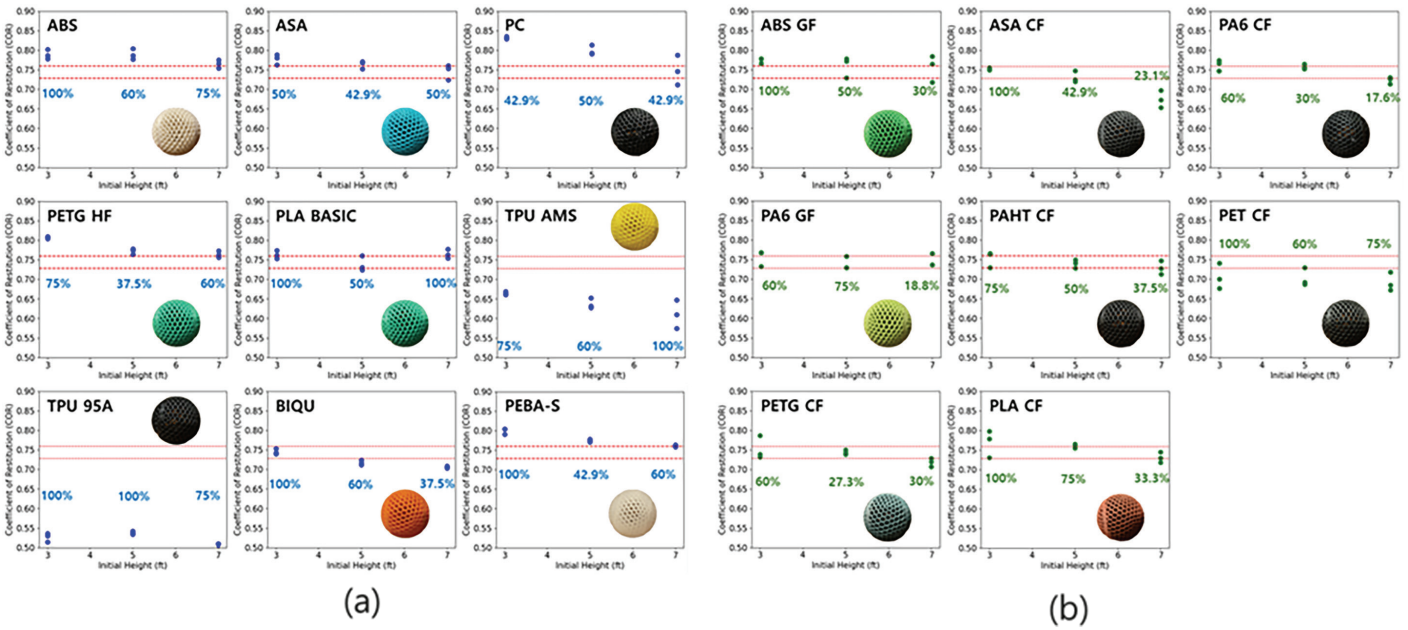

Figure 4. COR and success rates for airless tennis balls made from (a) non-reinforced and (b) fiber-reinforced (glass or carbon fiber) filaments. Dashed red line: average COR of reference tennis ball. Blue values: success rates. Success rates were measured by taking the ratio of successful trials to total trials, with a successful trial being one in which the ball rebounded roughly straight upwards.

cycle, tended to have higher COR. For example, PETG HF, ABS, and PLA Basic had higher damping times, above 3.0s, with higher COR values of 0.77–0.79. In contrast, TPU-based filaments (TPU AMS, TPU 95A) showed short damping times, less than 1.5 s, and lower COR values of less than 0.65, reflecting higher internal energy dissipation during deformation and rebound. This suggests that viscoelastic damping and internal friction significantly influence rebound efficiency (16). While longer damping times did generally yield higher COR, more extreme increases in damping times, such as BIQU (4.47 s, 0.72 COR) and PEBA-S (11.99 s, 0.78 COR), did not yield proportional increases in COR. Thus, other factors such as stiffness and mass distribution may also play significant roles in COR.

Figure 6b plots notched impact strengths against unnotched impact strength for each filament. As such, the filaments more closely clustered in the bottom left portion of the graph, closer to the origin are generally worse at withstanding sudden impacts. Dashed circles denote filaments which fractured during the drop test. Materials with both unnotched and notched strengths below ~35 kJ/m² and ~8 kJ/m², respectively—such as ASA CF, ABS GF, PLA Basic, PLA CF, PA6 GF, PC, PETG HF, and PET CF—were prone to fracture under repeated rebound testing. These materials tended to be stiff or brittle, limiting their ability to absorb impacts without breaking. In contrast, filaments with higher impact strengths— such as PAHT CF, ABS, ASA, PETG CF, PA6 CF— remained intact, indicating that surpassing these thresholds is critical for durability in airless tennis balls.

Figures 6c and 6d plot average success rate against Young's modulus and Tensile strength, respectively. Correlation analysis revealed a weak, negative correlation for both properties (−0.36 for Young's modulus and −0.44 for tensile strength). Softer materials (TPU 95A, TPU AMS, PEBA-S, BIQU; <1200 MPa) achieved >0.65 success rates, while stiff materials (PA6 CF, PAHT CF, ASA CF, PET CF; >3800 MPa) fell below 0.55. Similarly, materials with lower tensile strength (<50 MPa) often showed higher success rates—for example, TPU 95A, TPU AMS, and PLA Basic each exceeded 0.78 (Figure 6d). In contrast, very strong filaments (e.g., PA6 CF, >100 MPa) had the lowest success rate (0.36). These findings suggest that excessive material stiffness and strength may compromise rebound stability by concentrating stress

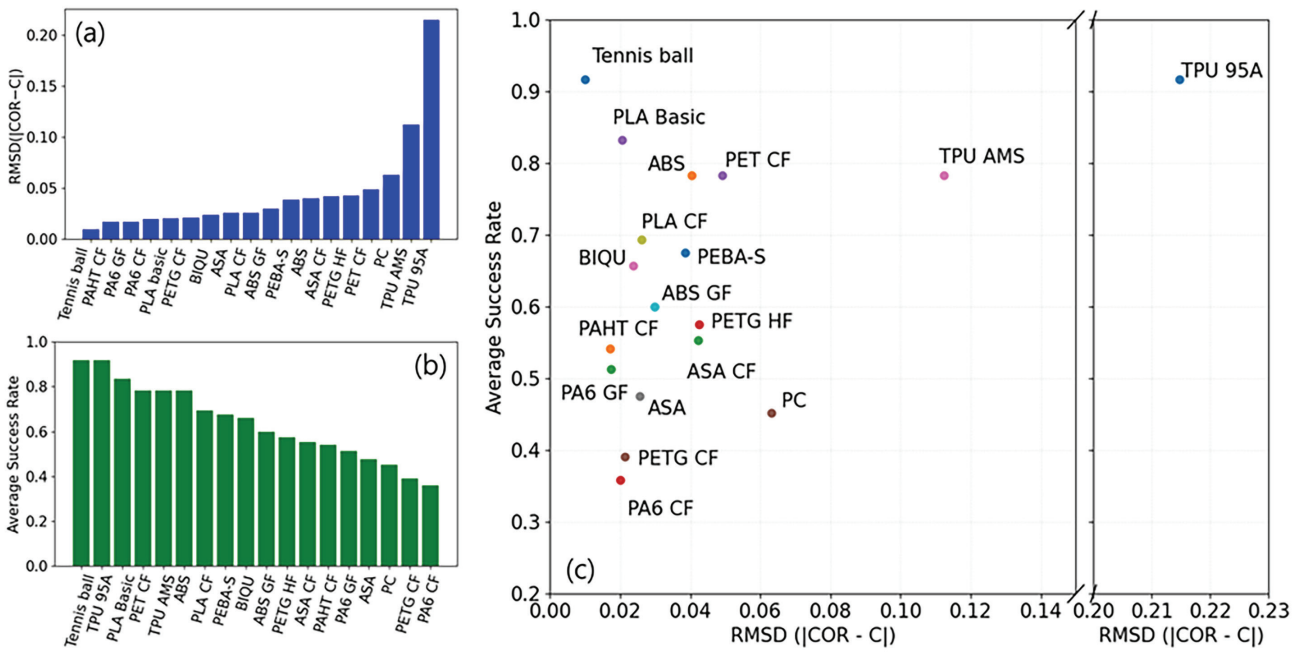

Figure 5. (a) RMSD(|COR−C|) for each filament. (b) Average success rate across drop heights. (c) Average success rate vs. RMSD(|COR−C|), showing general trends and outliers. Success rates were measured by taking the ratio of successful trials to total trials, with a successful trial being one in which the ball rebounded roughly straight upwards. RMSD(|COR−C|) is a measure of the average deviation of each trial from the official ITF COR value.

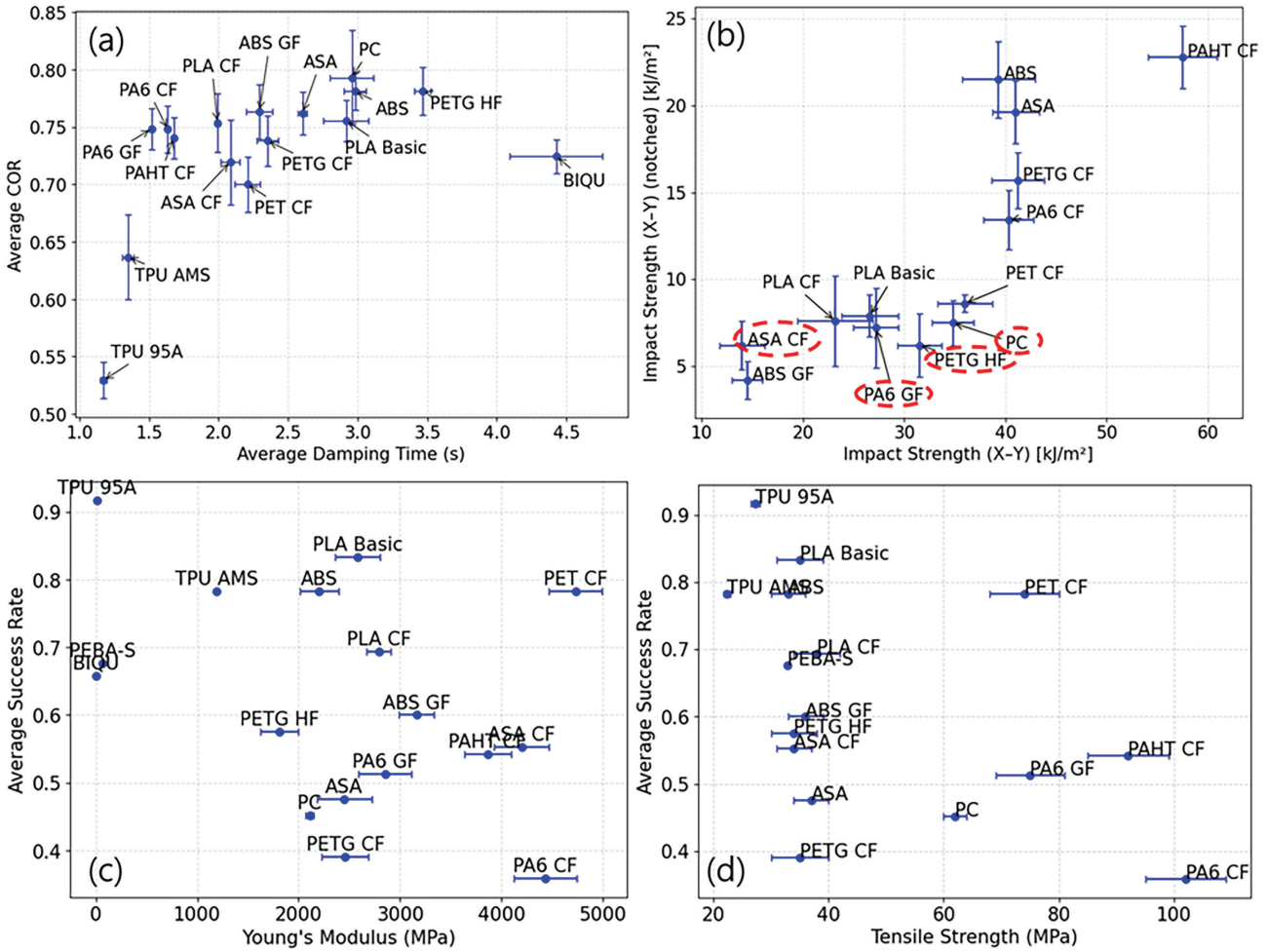

Figure 6. Effect of filament mechanical properties on airless tennis ball performance: (a) COR vs. damping time, (b) Charpy impact strength, with dashed circles indicating fracture during rebound tests, (c) Success rate vs. Young's modulus, and (d) Success rate vs. tensile strength. Charpy impact strength is used as a measure of a material's ability to resist sudden impacts before fracturing. Success rates were measured by taking the ratio of successful trials to total trials, with a successful trial being one in which the ball rebounded roughly straight upwards. Young's modulus is used as a measure of a material's stiffness— the amount of tension they can undergo in a certain direction before deformation. Damping time was used as a measure of a material's ability to dissipate energy. Tensile strength measures the amount of tension a material can undergo in a certain direction before complete fracture.

at small defects and limiting the material's ability to absorb and redistribute impact energy, thereby reducing rebound reliability.

However, several low-strength filaments, including ABS GF, PETG HF, ASA CF, ASA, and PETG CF, still showed relatively low success rates, indicating that tensile strength alone is not the only factor of print success. The results indicate that for airless tennis balls, materials of moderate stiffness and strength may be more desirable than materials that maximize these properties. High material stiffness and impact strength compromise rebound consistency, but low impact strengths can induce fractures.

RMSD(|COR−C|)−Success rate mapping

Figure 7 presents the same plot as Figure 5c, with the horizontal axis representing the RMSD(|COR−C|), and the vertical axis representing the average success rate. Filaments outlined by dashed circles either fractured during bounce testing, or are considered to be

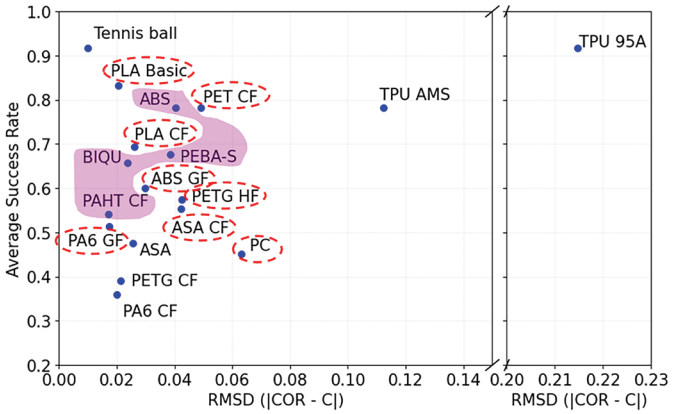

Figure 7. Two-dimensional performance map of tested filaments for airless tennis ball applications. RMSD(|COR−C|) is a measure of the average deviation of each trial from the official ITF COR value. Success rates were measured by taking the ratio of successful trials to total trials, with a successful trial being one in which the ball rebounded roughly straight upwards.

high-risk for fracture due to low impact strength. The shaded area marks filaments with an average success rate ≥ 0.50 and RMSD(|COR−C|) ≤ 0.05, indicating the filaments closest to the accepted success rate and RMSD(|COR-C|). Optimal candidates for airless tennis ball applications fall in the top left portion of the shaded region, where low RMSD(|COR−C|) values (< 0.05) coincide with high success rates. Materials with high RMSD(|COR−C|) values, such as TPU AMS and TPU 95A, produce rebound behavior starkly different from a standard regulation tennis ball, even if their success rates are relatively high. Conversely, filaments with low success rates (< 0.50) or those in the fracture-prone group are unsuitable for direct application without property modification, regardless of RMSD(|COR−C|) performance.

CONCLUSION

This study evaluated the performance of airless tennis balls fabricated from various commercial 3D printing filaments, focusing on the COR, rebound reliability (success rate), and fracture resistance. The key findings are as follows: 1) COR was most heavily determined by the material's damping characteristics. 2) Success rate showed a negative correlation with both Young's modulus and tensile strength. 3) Proneness to fracture was closely related to low impact strength.

For optimal performance, filaments should have a combination of moderate stiffness, low damping, and high impact toughness. Reinforced filaments such as CF or GF filaments, while providing high stiffness, generally exhibited reduced success rates and lower fracture resistance, making them less suitable for direct application. Future study should explore filament blending to balance stiffness and damping, as well as effects of internal ball geometry. Long-term durability under many repeated impacts should also be assessed.

ACKNOWLEDGEMENTS

I would like to acknowledge Mr. Mark Jedele for his invaluable mentorship and continuous support throughout this work.

CONFLICT OF INTERESTS

The author declares that there are no conflicts of interest regarding the publication of this article.

REFERENCES

1. Tadrist L & Darbois Texier B. Open questions on the impact of an inflated ball. arXiv preprint. 2017. Available from: https://arxiv.org/pdf/1708.01282 (accessed on 2025-08-13).
2. Cross R. Dynamic properties of tennis balls. Sports Engineering. 1999; 2 (1): 23-33. https://doi.org/10.1046/j.1460-2687.1999.00019.x
3. Wilson's New Airless Gen1 3D-Printed Basketball Hits the Market. Available from: https://3dprintingindustry.com/news/wilsons-new-airless-gen1-3d-printed-basketball-hits-the-market-228304 (accessed on 2025-08-13)
4. Filament for airless balls. Available from: https://forum.bambulab.com/t/filament-for-airless-balls/149585 (accessed on 2025-08-13). https://doi.org/10.4324/9781003585237-2
5. Airless soccer ball with TPU. Available from: https://forum.lulzbot.com/t/airless-soccer-ball-with-tpu/27239 (accessed on 2025-08-13)
6. Adli H & Ismail KA. Experimental investigation on restitution coefficient for sports balls. *IOP Conference Series: Materials Science and Engineering*. 2012; 36: 012038. https://doi.org/10.1088/1757-899X/36/1/012038
7. Skórski WW, Obszański M & Zawisza M. Experimental determination of the coefficient of restitution for selected modern hybrid composites. *Materials (Basel)*. 2021; 14 (19): 5638. https://doi.org/

10.3390/ma14195638

8. Willert E, Leroy J, Satora M & Scholtyssek Y. The influence of compressibility on the restitution coefficient for viscoelastic spheres in low-velocity normal impacts. arXiv preprint, 2018. Available from: https://arxiv.org/pdf/1806.06540 (accessed on 2025-08-13).
9. Airless Tennis Ball 2.0 Pickleball Wiffle. Available from: https://makerworld.com/en/models/253687-airless-tennis-ball-2-0-pickleball-wiffle (accessed on 2025-08-14)
10. Ashby MF. Materials Selection in Mechanical Design (5th ed.). Butterworth-Heinemann. 2017. ISBN: 978-0-08-100599-6.
11. Geier N, Davim JP & Szalay T. Advanced cutting tools and technologies for drilling carbon fibre reinforced polymer (CFRP) composites: A review. *Composites Part A: Applied Science and Manufacturing*. 2019; 125: 105552. https://doi.org/10.1016/j.compositesa.2019.105552
12. Parente JM, Silva AP & Reis PNB. The influence of carbon and glass fiber hybridization combined with a graphene-enhanced epoxy matrix on bending fatigue response. *International Journal of Fatigue*. 2025; 193: 108782. https://doi.org/10.1016/j.ijfatigue.2024.108782
13. Gao YF, Zhang W, Shi P., Ren WL & Zhong YB. A mechanistic interpretation of the strength-ductility trade-off and synergy in lamellar microstructures. *Materials Today Advances*. 2020; 8: 100103. https://doi.org/10.1016/j.mtadv.2020.100103
14. Hunt JF, Zhang H, Guo Z & Fu F. Cantilever beam static and dynamic response comparison with mid-point bending for thin MDF composite panels. *BioResources*. 2013; 8 (1): 115-129. https://doi.org/10.15376/biores.8.1.115-129
15. Weir G & McGavin P. The coefficient of restitution for the idealized impact of a spherical, nano-scale particle on a rigid plane. *Proceedings of the Royal Society A: Mathematical, Physical and Engineering Sciences*. 2008; 464 (2093): 1295-1307. https://doi.org/10.1098/rspa.2007.0289
16. Jian B, Hu GM, Fang ZQ, Zhou HJ, Xia R. Comparative behavior of damping terms of viscoelastic contact force models with consideration on relaxation time. *Powder Technology*. 2019; 356: 735-749. https://doi.org/10.1016/j.powtec.2019.08.110